---

**Article:**
Kim, B. orcid.org/0000-0002-7977-7845, Shin, Y. orcid.org/0000-0001-5865-3002, Park, S. et al. (4 more authors) (2025) Assessment of structural stability and leaching characteristics of phosphate-based geopolymer waste form containing radioactive spent ion exchange resins. Journal of Nuclear Materials, 607. 155671. ISSN: 0022-3115

https://doi.org/10.1016/j.jnucmat.2025.155671

---

Journal of Nuclear Materials

# Assessment of structural stability and leaching characteristics of phosphate-based geopolymer waste form containing radioactive spent ion exchange resins

--Manuscript Draft--

| | |
|---|---|
| **Manuscript Number:** | JNUMA-D-24-00822R1 |
| **Article Type:** | Full Length Article |
| **Section/Category:** | Radioactive waste materials |
| **Keywords:** | spent ion-exchange resin; phosphate-based geopolymer (P-GP); Immobilization; Radioactive waste; solidification; stabilization |
| **Corresponding Author:** | Wooyong Um<br>Pohang University of Science and Technology<br>Pohang, KOREA, REPUBLIC OF |
| **First Author:** | Byoungkwan Kim |
| **Order of Authors:** | Byoungkwan Kim |
| | Younglim Shin |
| | Solmoi Park |
| | Brant Walkley |
| | Seokyoung Oh |
| | Jaehyuk Kang |
| | Wooyong Um |
| **Abstract:** | The use of hydrated waste forms, such as cement, for immobilizing radioactive spent ion-exchange resins (IERs) is unsuitable due to low waste loading, high leaching of radionuclides, and poor durability. Here, simulant spent IERs were immobilized by a phosphate-based geopolymer (P-GP) for the first time. The 7-day compressive strength of the P-GP waste form was inversely proportional to waste loading because the pore size of the P-GP waste form increased with increasing waste loading. The P-GP waste forms with 40 wt% spent IERs satisfied all of South Korea's waste acceptance criteria for compressive strength, thermal cycling, water immersion, and gamma irradiation tests. The leaching behaviors of Co, Cs, and Sr differed from those of alkali-activated materials, but the leaching index exceeded the criterion value of 6.0. The leaching mechanism was governed by the combination of surface wash-off and diffusion or solely diffusion. The P-GP waste form could play as a primary physical barrier against releasing radionuclides. In addition, the geopolymer waste form did not undergo significant structural changes after waste acceptance criteria tests, indicating that it can efficiently immobilize spent IERs. Our findings can contribute new insights into efficient waste form materials for immobilizing radioactive spent IERs. |
| **Response to Reviewers:** | |

## Highlights

- **Radioactive spent ion exchange resins are immobilized using P-GP waste forms**
- **Pore structure changes in P-GP waste forms are investigated using TD-NMR**
- **Geopolymers with 40 wt% spent ion exchange resins meet the waste acceptance criteria tests**
- **P-GP waste forms show good durability after waste acceptance criteria tests**

Graphical Abstract

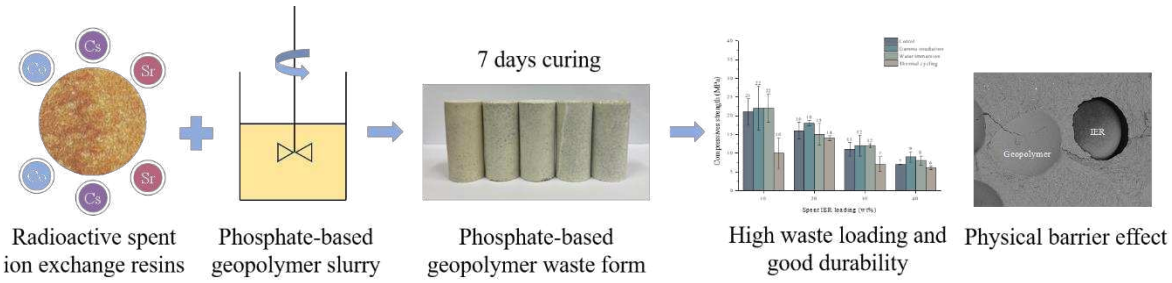


Radioactive spent ion exchange resins

Phosphate-based geopolymer slurry

Phosphate-based geopolymer waste form

High waste loading and good durability

Physical barrier effect

# Assessment of structural stability and leaching characteristics of phosphate-based geopolymer waste form containing radioactive spent ion exchange resins

Byoungkwan Kim[a,d], Younglim Shin[a,b], Solmoi Park[c], Brant Walkley[d], Seokyoung Oh[a], Jaehyuk Kang[a, e], and Wooyong Um[a, f, g, *]

[a] Division of Advanced Nuclear Engineering (DANE), Pohang University of Science and Technology (POSTECH), Pohang, Gyeongbuk 790-784, Republic of Korea

[b] Project Strategy Department, Korea Radioactive Waste Agency (KORAD), 19, Chunghyocheon-gil, Gyeongju-si, Gyeongbuk, Republic of Korea

[c] Department of Civil Engineering, Pukyong National University, 45 Yongso-ro, Nam-gu, Busan 48513, Republic of Korea

[d] School of Chemical, Materials and Biological Engineering, The University of Sheffield, S1 3JD, United Kingdom

[e] Department of Electrical and Energy Engineering, Jeju National University, 102, Jejudaehak-ro, Jeju-si, Jeju Special Self-Governing Province, 63243, Republic of Korea

[f] Division of Environmental Science and Engineering (DESE), Pohang University of Science and Technology (POSTECH), Pohang, Gyeongbuk 790-784, Republic of Korea

[g] Nuclear Environmental Technology Institute (NETI), Pohang University of Science and Technology (POSTECH), Pohang, Gyeongbuk 790-784, Republic of Korea

* Corresponding author: wooyongum@postech.ac.kr, Tel.:+82-54-279-9563, Fax:+82-54-279-9559

**Abstract**

The use of hydrated waste forms, such as cement, for immobilizing radioactive spent ion-exchange resins (IERs) is unsuitable due to low waste loading, high leaching of radionuclides, and poor durability. Here, simulant spent IERs were immobilized by a phosphate-based geopolymer (P-GP) for the first time. The 7-day compressive strength of the P-GP waste form was inversely proportional to waste loading because the pore size of the P-GP waste form increased with increasing waste loading. The P-GP waste forms with 40 wt% spent IERs satisfied all of South Korea's waste acceptance criteria for compressive strength, thermal cycling, water immersion, and gamma irradiation tests. The leaching behaviors of Co, Cs, and Sr differed from those of alkali-activated materials, but the leaching index exceeded the criterion value of 6.0. The leaching mechanism was governed by the combination of surface wash-off and diffusion or solely diffusion. The P-GP waste form could play as a primary physical barrier against releasing radionuclides. In addition, the geopolymer waste form did not undergo significant structural changes after waste acceptance criteria tests, indicating that it can efficiently immobilize spent IERs. Our findings can contribute new insights into efficient waste form materials for immobilizing radioactive spent IERs.

**Keywords: spent ion-exchange resin, phosphate-based geopolymer (P-GP), immobilization, radioactive waste, solidification/stabilization**

## 1. Introduction

In the nuclear industry, nuclear-grade ion-exchange resins (IERs) composed of macromolecular copolymers are conventionally used to purify various radioactive liquid wastes. Radionuclides with long half-lives (~30 years) such as $^{60}$Co (5.3 years), $^{90}$Sr (29 years), and $^{137}$Cs (30 years) are loaded in IERs, resulting in spent radioactive IERs. These radioactive spent IERs should be stabilized/solidified using suitable binder materials before being disposed of in a repository because they are considered low- and intermediate-level radioactive wastes (LILW). As assessed in December 2022, 13,969 drums (200 L) of spent IERs were stored temporarily in South Korea's nuclear power plants [1].

Conventionally, cementitious waste forms are used as binder materials to immobilize radioactive wastes owing to their low cost and simple solidification process [2]. However, several disadvantages of cementitious waste forms such as low leaching resistance and high porosity lead to their physicochemical degradation, resulting in high leaching of radionuclides [3, 4]. A major issue in using cement waste forms for immobilizing spent IERs is that they easily deteriorate owing to the swelling of spent IERs [5, 6]. The swelling of spent IERs due to water absorption can lead to the expansion of the binder matrix at an early age and affect the properties of the waste form such as its compressive strength, resulting in inferior immobilization performance [5, 6]. IERs immobilized in cementitious systems are prone to high volume changes because of the ion-exchange process and osmotic pressure variations [5, 7, 8]. In addition, spent IER loading in a cementitious waste form is relatively low at ~10 wt% [5, 9]. Therefore, additives such as natural pozzolanic material (zeolite) and clay (bentonite and vermiculite) are required to increase the loading of spent IERs up to 20 wt% in cementitious waste forms [5].

Furthermore, bitumen, polymer, and glass waste forms have been investigated as alternative matrices [10], among which the bituminous waste form (bituminization) has shown good immobilization performance, such as a high waste loading, low leaching rate, and low porosity [11]. However, bituminization requires several pretreatment processes of spent IERs under high temperatures (~200 ℃), which increase the cost of radioactive waste disposal and induce the generation of secondary gas wastes (e.g., CO(g), $CO_2$(g), and $SO_2$(g)) [11]. Solidification methods using thermosetting or thermoplastic polymers have advantages in terms of waste loading and leaching rate. However, the physicochemical stability of plastics is inferior to that of cementitious waste forms [11]. In polymer-based solidification, heterogeneous waste forms can be also generated due to the differences in density and weight between the polymer and spent IERs. Although the mechanical milling of spent IERs using a ball mill contributes to fabricating a homogeneous waste form with improved leaching stability, generating secondary radioactive wastes is also inevitable [12]. Further, borosilicate vitrification can be used to immobilize organic materials and volatile radionuclides such as $^{137}Cs$ [13, 14]. However, this process requires high-temperature (900-1,200 ℃) facilities, including a kiln, furnace, and melting apparatus [13].

Considering these aspects, a geopolymer waste form can be a suitable inorganic binder for solidifying spent IERs. Geopolymers are formed by polycondensation reactions between aluminate and silicate species released from precursors in an alkaline activator solution at a low temperature (<100 ℃) [15, 16]. The negative charge of the structure formed due to the substitution of [$SiO_4$] with [$AlO_4$] is compensated by monovalent cations ($Na^+$ or $K^+$), and the final reaction product is an amorphous solid phase [15, 16]. Several studies have demonstrated that geopolymers have attractive physicochemical characteristics such as a high early-age

compressive strength [17], high waste loading [18], and superior low leaching stability [19]. In particular, their immobilizing capacity for radioactive wastes such as contaminated soil [19], spent oil [20], sludges [18, 21], and borate waste [22] has been investigated. Aluminosilicate frameworks with a permanent negative charge are known to provide enough immobilization sites for binding cationic radionuclides via electrostatic interactions [23]. According to previous studies, spent IERs can be immobilized using a geopolymer with various precursor materials. Metakaolin-based geopolymer can immobilize up to 18 wt% of wet-based spent IERs and exhibit limited leaching rates for Cs and Sr [24]. However, during the geopolymer setting and hardening process, spent IERs may settle down to the bottom of the geopolymer waste form, resulting in a heterogeneous structure and poor durability [24]. Another study reported that the compressive strength of metakaolin-based geopolymer waste forms can be enhanced by reducing the spent IER loading [25]. For the fly ash-based geopolymer waste form, low spent IER loading (10 wt%), and low compressive strength (6.1 MPa) have been reported [26]. On the other hand, the ground granulated blast furnace slag-based geopolymer waste form, which is a calcium-rich system, can facilitate a high spent IER loading (wet-based 45 wt%) and meets the waste acceptance criteria tests in Taiwan [27]. Although the calcium-rich system has good characteristics, spent IERs containing boron generated after the treatment of borate streams are difficult to immobilize using calcium-rich binder materials like cement, because boron released from the IER hinders the hydration reaction [5]. Hence, low-calcium inorganic binder materials should be developed to immobilize spent IERs generated from various treatment processes.

Currently, phosphate-based geopolymers (P-GPs) fabricated by the phosphoric acid activation of a solid aluminosilicate material have attracted significant interest. The amorphous

aluminosilicate materials such as metakaolin can be activated with phosphoric acid to form an amorphous aluminosilicophosphate structure that includes Si-O-P, Si-O-Si, Al-O-P, and Si-O-Al linkages [28, 29]. Such materials are formed due to the generation of a phosphate unit, such as $P(OAl)_x(H_2O)_{4-x}$ [29]. Compared to alkali-activated systems (geopolymers and alkali-activated materials), P-GPs possess excellent characteristics, including a high compressive strength [29, 30] and high thermal stability [31]. Moreover, monovalent cations for charge compensations are not required due to the charge neutralization by the positive phosphorous unit. Thus, P-GP can be used to manage various hazardous wastes, including radioactive wastes.

In this study, P-GP was used as a waste form for the first time to immobilize simulant spent IERs. The waste acceptance criteria tests were also conducted to assess the structural stability of the resulting P-GP waste forms and the leaching behaviors of target radionuclides (Cs, Sr, and Co). In addition, pore structure variations owing to the immobilization of spent IERs and the effect of waste acceptance criteria tests on the structure of P-GP waste form were investigated.

## 2. Materials and methods

### 2.1 Preparation of simulant spent IERs and the P-GP waste form

For the preparation of an acidic liquid-waste simulant, iron chloride ($FeCl_3$, Sigma-Aldrich, 97%), chromium chloride hexahydrate ($CrCl_3 \cdot 6H_2O$, Acros Organics, 98%), manganese chloride tetrahydrate ($MnCl_2 \cdot 4H_2O$, Junsei Chemical, 98%), nickel nitrate hexahydrate ($Ni(NO_3)_2 \cdot 6H_2O$, Junsei Chemical, 97%), cobalt chloride ($CoCl_2$, Alfa Aesar, purity 97%), cesium chloride (CsCl, Sigma-Aldrich, 99.9%), and strontium nitrate ($Sr(NO_3)_2$,

Junsei Chemical, 97%) were dissolved in deionized water (DIW) at concentrations shown in Table 1. Cation–anion mixed IERs (IRN-150, Amberlite), which have been conventionally used in nuclear power plants in South Korea, were used to prepare the simulant spent IER. The mass ratio of the pure damp IER to acidic liquid waste was kept constant at 0.5, and the IER/acidic liquid waste mixture was stirred for 7 d for saturation in advance. After 7 d of saturation, the excess acidic liquid waste was removed by decantation. The saturated spent IER was sealed to prevent moisture evaporation and stored at room temperature. The concentrations of Co, Cs, and Sr in the acidic liquid waste before and after mixing with IERs were analyzed using an inductively coupled plasma-mass spectrometer (ICP-MS; NexION® 2000, Perkin Elmer) to confirm the amount of target radionuclides adsorbed to the IERs. Stable Co, Cs, and Sr isotopes were used as surrogates of $^{60}$Co, $^{90}$Sr, and $^{137}$Cs, and the adsorbed amounts of Co, Cs, and Sr were determined to be 0.48, 0.44, and 0.9 mg/g of the IER, respectively.

The P-GP waste forms were synthesized according to the formulations in Table 2 using commercial metakaolin (BASF), DIW, and an 85% phosphoric acid solution as starting materials. First, phosphoric acid and DIW were stirred for 2 h to prepare an acidic activator (10 M). Then, the geopolymer paste was prepared using a centrifugal mixer (ARE-310, Thinky Corporation, Japan). The mixing and de-gassing times were 4 min (1800 rpm) and 30 s (2100 rpm), respectively. The fresh slurry was cast in Φ30–H60 mm cylindrical molds. The P-GPs were agitated for 1 min to remove air bubbles and sealed with a plastic cover to prevent moisture loss. Thereafter, they were cured at 60 °C in an elect ric oven, according to the curing conditions in Table 2. The resulting P-GP waste forms were labeled according to their liquid-to-solid (L/S) ratio and spent IER loading (wt%). For instance, the P-GP waste form with an L/S ratio of 1.2 and waste loading of 50 wt% is denoted as 1.2G50.

## 2.2 Evaluation of waste acceptance criteria

Various tests, including compressive strength, thermal cycling, gamma irradiation, and water immersion tests, were conducted to assess the structural stability of the P-GP waste forms with spent IERs. The compressive strength of the P-GP waste form cured for 7 d was measured using a universal testing machine (ST-1001, made in South Korea) at a loading rate of 0.6 MPa/s. For thermal cycling tests, monolithic P-GP waste forms were positioned inside a temperature-controlled chamber, and the chamber temperature was first elevated to 60 ℃ and then lowered to −40 ℃ at the rate of 10 ℃/h. The chamber temperature was held for 1 h at the highest and lowest temperatures. This procedure was repeated 30 times over 1 month. The gamma irradiation test was conducted in a hanging tote gamma irradiation facility equipped with a $^{60}$Co source using a gamma-ray dose rate of approximately 1,851 Gy/h. The P-GP waste forms enclosed in an aluminum container at room temperature were irradiated until the cumulative minimum dose reached $10^3$ kGy, which lasted for 23 d. For water stability tests, the P-GP waste forms held using Teflon wires were immersed in DIW for 90 d. The DIW volume to P-GP surface area ratio (V/S ratio) was maintained at 10.0 ± 0.1 (634 ± 10 mL). After these tests, the compressive strength was also measured in triplicates.

The radionuclide (Co, Cs, and Sr) leaching behavior and the major element in the P-GP waste form (Si, Al, and P) were investigated by performing the ANSI/ANS 16.1 leaching test in triplicate [32]. The P-GP waste forms were submerged in DIW at a V/S ratio of 10.0 ± 0.1. The leachate was replaced with fresh DIW at 2 and 7 h, and at 1, 2, 3, 4, 5, 19, 47, and 90 d. The concentrations of Co, Cs, Sr, Si, Al, and P ions were analyzed using an ICP-MS. The effective diffusivity ($D_e$, cm$^2$/s) of various species was calculated as follows:

$$D_e = \pi \left[\frac{a_n/A_0}{(\Delta t)_n}\right]^2 \left(\frac{V}{S}\right)^2 T, \qquad (1)$$

where $a_n$ is the amount of species (mg) released from the P-GP waste form during leaching interval $n$, $A_0$ is the total quantity (mg) of a given contaminant in the P-GP waste form, $(\Delta t)_n$ is the leaching interval (s), $V$ and $S$ are the volume ($cm^3$) and surface area ($cm^2$) of the P-GP waste form, respectively, and $T$ is the leaching time (s) representing the "mean time" of the leaching interval.

When the amount of the removed species was more than 20%, $D_e$ was calculated as

$$D_e = \frac{Gd^2}{t}, \quad (2)$$

where $G$ is a dimensionless time factor for a cylindrical specimen that can be identified in a tabular manner, as determined by ANSI/ANS-16.1 [32]. Here, $d$ is the specimen diameter (cm), and $t$ is the elapsed leaching time (s)

The leachability index ($Li$) was calculated from the effective diffusivity using Equation (3).

$$Li = \frac{1}{n}\sum_{i=1}^{n}\left[log\left(\frac{\beta}{D_e}\right)\right]_i, \quad (3)$$

where $\beta$ is a defined constant (1.0 $cm^2/s$).

The cumulative fraction leached (CFL) and leaching rate were determined using Equation (4) and Equation (5), respectively.

$$CFL = \frac{\sum a_n}{A_0}, \quad (4)$$

$$Leaching\ rate = \left(\frac{\sum a_n}{A_0}\right)\frac{V}{S}\ \frac{1}{t}, \quad (5)$$

To further understand the leaching trends of radionuclides in the acid-activated geopolymer system and the physical barrier effect of the geopolymer waste form, 40 wt% of

the spent IER was immersed in an acidic activator required to make a 0.7G40 sample. The glass beaker containing the spent IER and an acidic activator was sealed to prevent water evaporation. Then, 8 mL of the acidic activator was collected at 2 and 7 h, and 1, 2, 3, 4, and 5 d intervals to analyze the concentrations of radionuclides using an ICP-MS.

**2.4 Leaching kinetic models**

Radionuclides of specific concern undergo a leaching process encompassing three stages: dissolution into the interstitial water, diffusion through this water to the surface of the waste matrix, and subsequent release into the saturated environment. A mathematical model, coupled with experimental data, can be employed to assess the leaching behavior of radionuclides transitioning from the immobilized waste matrix to the surrounding water [33, 34]. This is achieved by fitting experimental CFL data to distinct models: the first-order reaction model (FRM), the diffusion model, the first-order reaction/diffusion model (FRMDIF), the dissolution model, and the first-order reaction/diffusion/dissolution model (All) [33, 34].

The FRM is employed to estimate leaching parameters when radionuclide leaching is controlled by the exchange kinetics between the surface of the waste form and the leaching solution (wash- off). The surface exchange rate could be governed by a first-order reaction rate, thus being directly proportional to the amount of radionuclides present in the waste form as follow:

$$\frac{dQ}{dt} = kQ, \quad (6)$$

where, Q is the amount of radionuclides in the waste (mg/g) and k is a rate constant($s^{-1}$). The CFL is obtained using Equation (7).

$$CFL = Q_0(1 - \exp(kt)), \quad (7)$$

where $Q_0$ is the initial amount of target radionuclides in the P-GP waste form.

When migration of radionuclides is primarily governed by diffusion mechanism, the application of Fick's second law within a semi-infinite medium, in conjunction with Fick's first law, presents an approach to derive the flux of diffusing materials through the waste form as follow:

$$CFL = 2\left(\frac{S}{V}\right)\sqrt{\frac{D_e t}{\pi}}, \qquad (8)$$

The FRMDIF model is proposed for the release of radionuclides from the waste form influenced by both exchange kinetics between waste form surface and leaching solution, and diffusion. Thus, the CFL can be obtained by combining Equation (7) and (8):

$$CFL = Q_0(1 - \exp(kt)) + 2\left(\frac{S}{V}\right)\sqrt{\frac{D_e t}{\pi}}, \quad (9)$$

When a dominant element within the waste form constitutes the leaching species, its migration into the leaching solution initiates structural degradation of the matrix, referred to as dissolution, and can be calculated as follow:

$$CFL = \frac{S}{V}U_0 t, \quad (10)$$

where $U_0$ is the maximum network dissolution velocity.

The All model indicates that leaching results from the combined influence of the FRM, DIF, and dissolution models, as follow:

$$CFL = Q_0(1 - \exp(kt)) + 2\left(\frac{S}{V}\right)\sqrt{\frac{D_e t}{\pi}} + \frac{S}{V}U_0 t, \quad (11)$$

## 2.5 Test method for characterization

To investigate the pore structure changes in the P-GP waste form, time-domain nuclear magnetic resonance (TD-NMR) spectroscopy was conducted using an MQC-R NMR spectrometer (Oxford Instruments, made in England) operating at 20.82 MHz. The 90° pulse length was 4.04 μs. A pure geopolymer paste prepared with an L/S ratio of 2.0 and a 0.7G40 geopolymer paste were prepared because low L/S ratios increase the flowability and viscosity of the geopolymer paste. Freshly prepared geopolymer mixtures were poured into cylindrical NMR tubes and cured at 60 ℃ for 1 d in an electric oven. After they were hardened, their spin–spin relaxation time and solid fraction were measured once a day for 5 d. The liquid water signals were resolved into different $T_2$ components by employing the Carr–Purcell–Meiboom–Gill (CPMG) sequence. The number of echoes was 1024, and the repetition time was 1000 ms. The average number was 128 and 64 for CPMG and quadrature echo, respectively. The quadrature echo signals were obtained from the samples at multiple pulse gaps ($\tau$) in the range of 12 to 45 μs, and the signals were deconvoluted into Gaussian and exponential decay functions to quantify the solid and liquid water, respectively. The contribution of the bound water (solid fraction) to the signal was determined by extrapolating the Gaussian part to the zero-pulse gap. The micro morphologies of the P-GP waste forms sputter-coated with Pt were observed using a field-emission scanning electron microscope (FE-SEM; JEOL JSM-7800F, Japan) equipped with a back-scattered electron detector (BSE) at 20 kV acceleration voltage.

A Rigaku MiniFlex instrument (Japan) was used to perform X-ray diffraction (XRD) of the P-GP waste forms. The XRD patterns were obtained in the range of $10° \leq 2\theta \leq 60°$ at 0.02° step size. The operating current and voltage were 15 mA and 40 kV, respectively. The crystalline phase was identified using “PDF-2” and “PDXL” software. The chemical structure

of the P-GP waste form was investigated using a Fourier-transform infrared (FT-IR) spectrometer (Nicolet iS10 spectrometer, USA) in the attenuated total reflection mode. The FTIR spectra were collected in the wavenumber range of 600–4000 $cm^{-1}$.

## 3. Results

### 3.1 Effect of the L/S ratio on the mechanical characteristic of the P-GP waste form

The P-GP waste form prepared using an L/S ratio of 1.2 showed the highest 7-day compressive strength of 73 MPa, and the compressive strengths of the P-GP waste forms decreased with increasing loading of the spent IER (Table 3). All P-GP waste forms loaded with spent IERs met the waste acceptance criterion for compressive strength (3.445 MPa), except for the sample with 50 wt% spent IERs. Notably, no swelling or visible cracks were observed in the prepared P-GP waste forms. The reduction in the compressive strength with increasing IER content is related to the structural characteristics of the IER which has a low mechanical strength owing to its highly porous structure [35], because the IERs are known to reduce the compressive strength of binder materials such as cementitious waste forms [5]. In addition, physically encapsulated spent IERs leave microcracks and holes in the solidified matrix, resulting in low mechanical stability of the waste form [36]. A high L/S ratio also adversely affected the compressive strength (Table 3). The simulant spent IERs used in this study were in a water-saturated state (e.g., resin slurry), and the surface of IER particles can contain free-standing water adsorbed via electrostatic forces [9]. Thus, the actual L/S ratio would be higher than the stoichiometric L/S ratio used in formulation of geopolymer waste form. The water content is one of the critical parameters that determine the physical characteristics of the P-GP waste form [37]. Thus, the high free water content increased the

setting time and decreased the compressive strength of the P-GP waste form. This is because the additional water from the spent IERs can dilute the phosphoric acidic activator, leading to a disordered microstructure of the geopolymer [37]. To further analyze the effect of the water content, P-GP waste forms prepared using different L/S ratios and spent IER loadings were evaluated (Table 2). Based on empirical experiments, the L/S ratio of the geopolymers loaded with low (10–20 wt%) and high (30–50 wt%) quantities of the spent IER was kept constant at 1.0 and 0.7, respectively. The reduction in the L/S ratio contributed to improved compressive strength and the compressive strength of the geopolymer with the highest spent IER exceeded 3.45 MPa (Table 3). These results indicate that the free or mixing water content of the geopolymer waste form should be optimized according to the spent IER loading to obtain durable waste forms. According to a previous study, the 28-day compressive strength of a cement waste form with 15 wt% water-saturated spent IER was ~10 MPa [27]. The P-GP waste forms prepared in this study showed comparable compressive strengths to those of cement waste forms, despite a shorter curing time and higher spent IER loading (Table 3) [27].

TD-NMR analyses were conducted to understand the effect of the spent IER on the pore structure of the P-GP waste form and the corresponding change in the compressive strength. The results indicated that the spent IER significantly affected the pore structure of the P-GP waste form. The different forms of water in a geopolymer can be identified using the relaxometry spectrum ($T_2$ relaxation time distribution map), which is depicted in Fig. 1a and c. The measured relaxation times provide information on water species present in various pore populations or pores of different sizes in hydrated materials such as cement and geopolymers. For a geopolymer system, a shorter $T_2$ time correlates to water molecules strongly bound to its structural units (~0.1 ms), whereas a longer $T_2$ time represents the free water molecules in its gel and capillary pores (>1 ms) [29, 38-40]. The pristine geopolymer without the spent IER

exhibited a major asymmetrical peak at $2.0\times10^{-5}$ s, which became broader and shifted to a longer relaxation time of $4.45\times10^{-5}$ s at the highest amount of the incorporated spent IERs. This is possibly because the spent IER slightly increased the pore size of the geopolymer, as the $T_2$ relaxation time becomes longer as the pore size increases [41]. Further, two distinct peaks were observed at longer relaxation times (0.001–0.01 s) for the geopolymer containing the spent IER; these peaks were attributed to free water in gel pores and large capillaries (Fig. 1a and c). These results are consistent with the $T_2$ relaxation time of spent IERs which showed distinct peaks at similar $T_2$ time (Fig 1c). The appearance of these peaks indicates that heterogeneous and porous microstructures can be formed along the contact zone between the spent IERs and hydrated binder material such as $C_3S$ cement and cement-metakaolin blended waste forms [8, 42]. In addition, the free-standing water on the water-saturated spent IER surface acted as the initial free water in the geopolymer paste. It increases the free water content of the geopolymer slurry, leading to increased porosity and decreased compressive strength of the P-GP waste form [37]. Thus, spent IERs can increase the free water content of P-GP waste forms and affect their pore structure. The bound water content of spent IERs was approximately 6.05%, while the bound water content of P-GP waste form including spent IER, was about 6 to 10% higher than that of pristine P-GP (Fig. 1b and d). The bound water content represents the water in the calcium silicate hydrated interlayer and hydrated protons incorporated into hydrated minerals such as ettringite $Ca_6Al_2(SO_4)_3(OH)_{12}\cdot26H_2O$ and portlandite ($Ca(OH)_2$) [40]. However, hydrated mineral phases of calcium cannot be formed in our geopolymer system, because it is a calcium-free system and its formation mechanism is a polycondensation reaction and not a hydration reaction. Therefore, we infer that bound water of P-GP represented physically or chemically bound water in aluminophosphate structure (e.g., $P(OAl)_x(H_2O)_{4-x}$) of P-GP waste form and the increased solid fraction signals were originated from free-standing water present in water-

saturated IER particles (Fig. 1b and d). The increase in the pore size and free water content contributed to the decrease in the compressive strength of the spent IER-loaded P-GP waste forms.

### 3.2 Structural stability of the P-GP waste forms

According to the waste acceptance criteria of a LILW disposal facility in South Korea, relevant tests such as gamma irradiation, water immersion, and thermal cycling tests, were performed on all waste forms, except for the 0.7G50 geopolymer, because its compressive strength barely exceeded 3.45 MPa (Table 3). The gamma irradiation test slightly increased the compressive strength of the samples; however, the increases are not significant, considering the standard deviation ranges (Fig. 2). According to a previous study, gamma irradiation can change certain physical characteristics of cementitious materials such as their compressive strength, average pore diameter, and microstructure [43]. The compressive strength of a cement matrix decreased by up to 15% because of the radiolysis of the pore water and hydration reaction products (e.g., hydrated mineral phases) [43]. Similar pore water radiolysis occurs in geopolymers. Generally, the water content in alkali-activated geopolymer waste forms, which use metakaolin as a precursor, is higher than that in cement (above 30 wt%); however, the amount of $H_2$ gas, which is potentially generated from the radiolysis of water in a geopolymer, is lower than that observed in cement waste forms [44]. These results are due to the different pore solutions and pore structures of the cement and geopolymer; for instance, the pore solution characteristics of a geopolymer such as the ionic constitution and pH, may vary depending on the raw materials and alkaline activator types [44, 45]. In other words, geopolymers have better gamma radiation resistance than cement. This is presumably because geopolymers do not form a structure via hydration reactions and water is physically trapped in their pores. When gamma

rays are irradiated on a cement waste form, not only the pore water but also the water present in the hydrate reaction products undergo radiolysis, leading to decreased compressive strength [43]. On the other hand, for a geopolymer, even if the pore water is radiolyzed during gamma irradiation, it does not have a significant effect on the amorphous structure of the geopolymer, which contributes to the compressive strength of the sample, and the gamma ray slightly increases the compressive strength by densifying the Si-O bonds [44]. The free water content of the P-GP waste form used in this study is approximately 17–23 wt%, significantly lower than that of the cement waste form with a water-to-cement ratio of 0.4 (28 wt%) [44, 46]. In addition, an amorphous structure of P-GP waste forms is formed through polycondensation reactions, rather than hydration reactions [28]. In this study, the compressive strength of the P-GP waste form did not change significantly after gamma irradiation, indicating its good resistance to gamma irradiation, similar to those of alkali-activated geopolymers.

Furthermore, no physical degradation of the P-GP waste forms or reduction in their compressive strength occurred after the water immersion test, considering the standard deviation, regardless of the spent IER loadings (Fig. 2). The previous study reported that immersion in water reduced the compressive strength of P-GP from 88 to 41 MPa in 28 d [47]. The significantly different behavior of our system could be related to the hydrolysis of the Si-O-P units in the geopolymer [48]. A previous study suggested that less than 10% of Si-O-P units could be formed during geopolymerization reaction because silicate species have low reactivity in low-pH environments [28]. The number of Si-O-P units gradually decreased with increasing spent IER loading because of the decrease in the metakaolin content, the precursor of Si-O-P units. Therefore, it can be inferred that the number of Si-O-P units affected by hydrolysis is reduced, and thus, there is no significant change in the compressive strength of the P-GP waste form after the water immersion test.

No notable cracks were found on the surfaces of the P-GP waste forms after the thermal cycling test. However, this test negatively affected their compressive strength (Fig. 2). In particular, the compressive strength of the P-GP waste form loaded with 10 wt% spent IER decreased by ~52% (from 21 to 10 MPa; Fig. 2). In the different spent IER loadings, the compressive strength decreased by less than 37%. The thermal cycling conditions can enhance or deteriorate the physical characteristics of the geopolymer, depending on the type of the radioactive waste. For a P-GP waste form used to immobilize borate waste, the compressive strength after thermal cycling increased from 15 to 22 MPa, and the total porosity of P-GP waste form decreased from 31 to 20% [49]. This is because additional heat curing occurs during thermal cycling at 60 °C which enhances the physical characteristics of P-GP waste form. Further, the compressive strength of a P-GP waste form loaded with organic liquid radioactive waste (spent tributyl phosphate and kerosene) decreased by up to 24% after freeze and thaw cycles [50]. The detailed mechanism was however not clearly investigated, and the decreased compressive strength was speculated to be related to the L/S ratio of the geopolymer waste form. Apparently, the addition of liquid radioactive waste increased the L/S ratio, negatively affecting the structure of the P-GP waste form during the freeze period. The volume expansion of free water during the freezing cycle can induce microcracks and decrease the compressive strength. The results of the present study can be attributed to the freezing and thawing of the free-standing water held between the IER particles via electrostatic interactions because the freeze cycle does not affect the physical stability of the IER [51]. Thus, the decreased compressive strength after thermal cycling test is likely caused by increased free water content due to the loading of the water-saturated IER. Compared to the cement waste form, the P-GP waste form is expected to be a better binder material to immobilize spent IERs because approximately four times higher waste can be loaded into it and all waste acceptance criteria

are satisfied.

### 3.3 Leaching behaviors of Co, Cs, and Sr in the P-GP waste forms

The leached amounts of P, Al, and Si, which are the major elements that constitute the P-GP waste form (0.7G40 sample), were extremely low (Fig. 3). The highest CFL of 0.01% ± 0.005% was found for Si, and the CFL values of P and Al were 0.004% ± 0.0002% and 0.0008% ± 0.0001%, respectively (Fig. 3). The leaching rates of the Si, Al, and P were fast in the initial leaching period (< 5 days) and then gradually decreased (Fig. 3). These results revealed that the major elements which form the core building units of the geopolymer binder rarely leached, suggesting that the geopolymer has good leaching stability, although it contains a high quantity of the spent IER. On the other hand, the radionuclides (Co, Cs, and Sr) present in the spent IER leached to some extent from the P-GP waste form. The CFL values of Co, Cs, and Sr were 24.5% ± 1.78%, 15.4% ± 3.3%, and 3.8% ± 0.8%, respectively. The leachability indices of Co, Cs, and Sr were 8.6% ± 0.4%, 8.9% ± 0.2%, and 10.5% ± 0.4%, respectively, which met the waste acceptance criteria of 6.0 set by the ANSI/ANS16.1 [32].

Several studies have investigated the leaching behaviors of Cs and Sr in alkali-activated geopolymer waste forms loaded with spent IERs. The blast furnace slag-based geopolymer waste form used to immobilize spent IERs showed low CFL values for Cs (10.4%) and Sr (0.06%) [27]. The metakaolin-based geopolymer waste form containing 12 wt% spent IER had a high leachability index for Cs (13.71) and Sr (12.12), depending on the mix formulation [24]. However, it is difficult to compare the leachabilities directly because previous studies activated the raw materials using an alkaline activator such as a sodium silicate solution to fabricate geopolymer waste forms. Alkali-activated geopolymers electrostatically attract the cations owing to their permanent negative charges [16, 52]. In contrast, the P-GP has a weak

electrostatic interaction with the cations because it is neutral or positively charged depending on the P/Al molar ratio [53, 54]. The alkaline activation solution has a high pH and high $OH^-$ concentration, whereas the acidic activation solution with a low pH has a high $H^+$ concentration. The adsorbed Co, Cs, and Sr ions in the spent IER incorporated in the P-GP waste form can be easily released by ion exchange with protons because a strong acidic activator is used to fabricate the P-GP waste form. Therefore, the leaching mechanism of the spent IER in the P-GP waste form should be evaluated comprehensively. To better understand the leaching behaviors of Co, Cs, and Sr in the acid activation system, a quantity equivalent to 40 wt% of the spent IER was immersed in an acidic activator required to fabricate a geopolymer waste form with an L/S ratio of 0.7. The results revealed a similar trend of the leaching results to that of the geopolymer waste form in DIW (Fig. 3). The CFL was approximately 78.7% and 73.6% for Co and Cs, respectively (Fig. 4). The CFL for Sr was ~28.4%, approximately three times lower than those of Co and Cs. Overall, the leaching rates of the radionuclides were fast in the early leaching periods (during 1 d) and then gradually decreased (Fig. 4). These results reveal that Co, Cs, and Sr in the spent IER can be released using an acidic activator. The geopolymer waste form acts as a primary barrier that prevents the leaching of the radionuclides from the spent IER. The ion exchange capacity depends on several factors such as the electrical charge of the ion (valence of ions), ion concentration in the solution, and physicochemical characteristics of the ions [55]. The ion exchange affinity is proportional to the electrical charge and the atomic number of targeted ions [55]; for instance, the affinity of cations is high in the order of Sr, Co, and Cs. In other words, theoretical CFL will be higher in the order of Cs, Co, and Sr, but the CFL of Co was higher than that of Cs in this study (Fig. 3). This may be explained by the concentration and dissolution of Co. The specimen contained a large amount of Co that could be released because the initial concentration of Co was more than twice that

of Cs. Another possible hypothesis for this result is the dissolution of Co by the phosphoric acid activator [56]. Phosphoric acid can be used as an efficient leaching and precipitating agent to recover Co from wastes (e.g., lithium cobalt waste) and cobalt phosphate ($CO_3(PO_4)_2$) can be precipitated, as shown in Equation (8) [56]:

$$Co^{2+}(aq) + Li^{+}(aq) + PO_4^{3-}(aq) = 1/3Co_3(PO_4)_2(s) + 1/3Li_3PO_4(s) \quad (8)$$

Further, the precipitated cobalt phosphate can be dissolved under excessive phosphoric acid conditions, as follows:

$$Co_3(PO_4)_2(s) + 12H^{+}(aq) + 4PO_4^{3-}(aq) = 3Co^{2+}(aq) + 6H_2PO^{4-}(aq) \quad (9)$$

The Co exchanged and released from the spent IER can exist as $Co^{2+}$ in the P-GP waste form because Co forms $Co^{2+}$ ions in an acidic environment. Thus, a part of the liberated Co ions was precipitated as cobalt phosphate in the P-GP waste form and then continuously dissolved under the strongly acidic condition, resulting in a high CFL and low leachability index when tested using an acidic activator.

The kinetic leaching models were employed to investigate various leaching behaviors, including surface wash-off, diffusion, or dissolution. Upon examining Fig. 5, it can be concluded that, for Co and Sr, the FRMDIF model better fitted the experimental data compared to the FRM, dissolution, and combination models. Other models resulted in significant underestimates or overestimates of CFL for Co and Sr. This indicates that conceptual models based on single leaching mechanisms (FRM, diffusion, and dissolution) inadequately represented the leaching behavior of Co and Sr during the experimental period. Generally, the FRMDIF model proved to be the most suitable for describing the leaching behavior of Co and Sr in geopolymer waste forms. The FRMDIF model suggested that soluble compounds might rapidly leach out initially, with the dissolution rate being controlled by the initial surface wash-off effect. After surface wash-off, less soluble compounds could penetrate the porous matrix

through diffusion. Conversely, the fitting results of CFL for Cs exhibited a higher correlation coefficient for the diffusion model compared to other models. This suggests that Cs transport in a geopolymer waste form is predominantly controlled by a single leaching mechanism, such as diffusion. Interestingly, the leaching model fit results for CFL in the IER acid immersion test revealed differential leaching behavior. The leaching of Co and Sr were governed by the diffusion model, while Cs followed a combination model involving surface wash-off, diffusion, and dissolution, rather than a single leaching mechanism. Considering this along with the results of IER acid immersion test (Fig. 4), mechanism of the radionuclides released from the IER was influenced by the geopolymer waste form playing a primary physical barrier role that immobilized the IER. The amorphous geopolymer structure which has a compact microstructure physically retains the leaching and diffusion of radionuclides.

### 3.4 Effect of waste acceptance criteria tests on the P-GP waste form structure

SEM, XRD, and FT-IR analyses were conducted on the 0.7G40 sample to understand the effect of the waste acceptance criteria tests on the geopolymer structure. These waste acceptance criteria tests did not induce significant changes in the microstructure of the geopolymer (Fig. 6). The SEM-BSE micrographs of the P-GP waste form subjected to waste acceptance criteria tests revealed that the spent IERs were covered with the geopolymer binder and they were physically encapsulated in the geopolymer waste form (Fig. 6). Furthermore, microcracks were observed in both the geopolymer binder and the spent IERs. It may be attributed to microcracking during the compressive strength measurement or cracking due to dehydration during SEM sample preparation (Pt coating) or loading the sample into the vacuum chamber for SEM analysis. The porous voids between the spent IER particles and geopolymer matrix were confirmed, which indicated that the spent IER particles were physically

immobilized. This is because the organic IER did not react with the inorganic binder matrix [8, 42].

For XRD and FT-IR analyses, geopolymer fractures obtained after the compressive strength test were ground and passed through a 200-mesh screen (0.075 mm) to remove the spent IER. The thermal cycling and water immersion tests did not affect the crystallographic structure, and no new crystalline phases were observed. The XRD patterns of all P-GP waste forms exhibited a broad asymmetric amorphous hump at $2\theta$ = 18–30° (Fig. 6), which is attributed to the amorphous structure of the geopolymer [28]. On the other hand, gamma irradiation led to the formation of a crystalline aluminum phosphate phase ($AlPO_4$, PDF #01-074-3256) (Fig. 7). A low gamma ray dosage (1,574 kGy) allows the recrystallization of the amorphous phase in the geopolymer [57]. The reflection at $2\theta$ = ~26° is attributed to the impurity of metakaolin (anatase, $TiO_2$) [22]. The FT-IR spectra confirmed that the tests did not affect the molecular bonding structure of the geopolymer waste forms (Fig. 8). The broad asymmetric peak at 960–1270 $cm^{-1}$ is assigned to the Si-O-Al-O-P and Si-O-Si bonds in the geopolymer [28, 29]. Further, the weak peak at 790 $cm^{-1}$ is due to the stretching vibrations of the Si-O-Si bonds [28, 29]. These results indicate that the aluminosilicate structure of metakaolin was transformed into aluminosilicophosphate and amorphous silica phases under acidic activation [28, 29]. The peaks appear at the wavenumbers of 3300 and 1640 $cm^{-1}$ which correspond to the stretching of O-H and vibration of H-O-H, respectively [28, 29]. In other words, the P-GP waste form could withstand abnormally aggressive conditions, such as a radioactive waste repository environment. Considering these results, the P-GP waste form is suitable for immobilizing spent IERs, which are challenging to stabilize/solidify using cementitious and alkali-activated materials, and it tolerates a high waste loading and exhibits good physicochemical performance.

## 4. Discussion

As previously described, radioactive spent IERs are among the most challenging radioactive wastes to immobilize for disposal due to their tendency to swell upon contact with water, leading to the degradation of the waste form. The previous studies have utilized methods like drying and grinding spent IERs into powder [12] or thermal decomposition at 450 ℃ to ash for immobilization [58]. While these improve physicochemical properties, they produce significant secondary radioactive waste (e.g., spent filters, grinders, and dust). In addition, the high radiation levels in spent IERs pose the health risks for workers during these processes. Therefore, it is crucial to develop waste forms with excellent physicochemical immobilization performance while minimizing the processing of radioactive spent IERs.

Our research demonstrates that saturating radioactive spent IERs with water before immobilization can be an efficient disposal method that requires minimal pretreatment. The bound water by electrostatic forces in the water-saturated spent IERs functions like the free water in geopolymer, enlarging the pore structure and reducing compressive strength (Fig. 1 and Table 3). However, optimizing the mixing water content of P-GP waste form according to the waste loading of spent IERs can achieve higher compressive strength and a higher waste loading. Furthermore, results indicate that P-GP waste forms can be used as a binder material for radioactive waste disposal at the LILW disposal facility in South Korea. The P-GP waste form loaded with spent IERs met the compressive strength criterion (3.445 MPa) even after thermal cycling, gamma irradiation, and long-term immersion tests, maintaining durability without significant changes in the matrix structure (Fig. 2, 6, and 7). Although the positive surface charge of the P-GP waste form resulted in slightly lower immobilization capability for target cationic radionuclides (Co, Cs, and Sr) compared to alkali-activated geopolymers which have the permanently negative surface charge, the Li for radionuclides still met the criteria

(>6.0), indicating sufficient leaching resistance for practical use (Fig. 3). Additionally, leaching tests focused only on cationic radionuclides with established waste acceptance criteria; however, actual radioactive spent IERs may adsorb a variety of anionic radionuclides. This is because mix bed IRN-150, which consists of both cation exchange resins and anion exchange resins, is widely used in nuclear power plants. A recent study has reported that the positive surface charge of P-GP can efficiently immobilize anions such as Se and I through electrostatic attraction [59]. Since alkali-activated geopolymers have very weak immobilization capabilities for anions, using P-GP could enable more efficient immobilization of anionic spent IERs and radioactive anions [59].

Recently, P-GP has been widely used in various fields such as construction materials, ceramics, and environmental applications. However, research related to radioactive waste disposal using P-GP is very limited. This is likely because P-GP research is still in its early stages. The results of our study demonstrate that P-GP can be effectively used for the disposal of radioactive waste that is difficult to dispose of with cement or alkali-activated geopolymers. This research can provide a basis for the disposal of various types of radioactive waste that will be produced during the decommissioning of nuclear power plants in the future, as well as for radioactive waste that is challenging to dispose of using hydrated waste forms with alkaline systems.

## 5. Conclusion

The P-GP waste forms were fabricated at various L/S ratios to immobilize spent IERs and waste acceptance criteria tests were conducted to assess their structural stability. The maximum spent IER loading (40 wt%) was achieved at an L/S ratio of 0.7, and the 7-day compressive strength test results of the resulting P-GP waste form satisfied the compressive strength

criterion of 3.45 MPa. The TD-NMR results also revealed that the spent IERs slightly increased the pore size and free water content of the P-GP waste form, reducing its compressive strength. Nevertheless, the compressive strengths of all P-GP waste forms exceeded 3.45 MPa after the waste acceptance criteria tests. The 90-days leaching test results confirmed that the main elements of the P-GP waste form (Si, Al, and P) barely leached. The leachability indices of Co, Cs, and Sr were higher than the 6.0 set by the ANSI/ANS16.1 test, and the controlling leaching mechanism was FRMDIF or diffusion. Analyses of SEM, XRD, and FT-IR confirmed that the waste acceptance criteria tests did not induce structural changes in the P-GP waste form. The findings of this study suggest that the P-GP waste form can be a suitable binder material for efficiently immobilizing radioactive spent IERs, which are challenging to dispose of as cement and alkali-activated waste forms.

**Acknowledgment**

This work was supported by the Institute for Korea Spent Nuclear Fuel (iKSNF) and Korea Foundation of Nuclear Safety (KOFONS) grant funded by the Korea Government (Nuclear Safety and Security Commission, NSSC) (No. 2109092–0323-SB120).

**References**

[1] Korean Association for Radiation Protection, Status of Radioactive Waste Management and Technology Development, Winter Workshop I, 2023.

[2] J.F. Li, L. Chen, J.L. Wang, Solidification of radioactive wastes by cement-based materials, Prog. Nucl. Engery, 141 (2021) 103957, https://doi.org/10.1016/j.pnucene.2021.103957.

[3] J.G. Jang, S.M. Park, H.K. Lee, Physical barrier effect of geopolymeric waste form on diffusivity of cesium and strontium J. Hazard. Mater., 318 (2016) 339-346,

https://doi.org/10.1016/j.jhazmat.2016.07.003.

[4] J.Y. Goo, B.J. Kim, M. Kang, J. Jeong, H.Y. Jo, J.S. Kwon, Leaching Behavior of Cesium, Strontium, Cobalt, and Europium from Immobilized Cement Matrix, Appl. Sci., 11 (2021) 8418, https://doi.org/10.3390/app11188418.

[5] R.O. Abdel Rahman, M.I. Ojovan, Toward Sustainable Cementitious Radioactive Waste Forms: Immobilization of Problematic Operational Wastes, Sustainability, 13 (2021) 11992, https://doi.org/10.3390/su132111992.

[6] J. Li, J. Wang, Advances in cement solidification technology for waste radioactive ion exchange resins: a review, J. Hazard. Mater., 135 (2006) 443-448, https://doi.org/10.1016/j.jhazmat.2005.11.053.

[7] E. Lafond, C.C.D. Coumes, S. Gauffinet, D. Chartier, L. Stefan, P. Le Bescop, Solidification of ion exchange resins saturated with Na+ ions: Comparison of matrices based on Portland and blast furnace slag cement, J. Nucl. Mater., 483 (2017) 121-131, https://doi.org/10.1016/j.jnucmat.2016.11.003.

[8] E. Lafond, C.C.D. Coumes, S. Gauffinet, D. Chartier, P. Le Bescop, L. Stefan, A. Nonat, Investigation of the swelling behavior of cationic exchange resins saturated with Na+ ions in a C3S paste, Cem. Concr. Res., 69 (2015) 61-71, https://doi.org/10.1016/j.cemconres.2014.12.009.

[9] J.S. Shon, H.K. Lee, T.J. Kim, J.W. Choi, W.Y. Yoon, S.B. Ahn, Evaluation of Utility of the Cement Solidification Process of Waste Ion Exchange Resin, Toxics, 10 (2022) 120, https://doi.org/10.3390/toxics10030120.

[10] B.K. Singh, M.A. Hafeez, H. Kim, S. Hong, J. Kang, W. Um, Inorganic waste forms for efficient immobilization of radionuclides, ACS ES&T Engineering, 1 (2021) 1149-1170, https://doi.org/10.1021/acsestengg.1c00184.

[11] J.L. Wang, Z. Wan, Treatment and disposal of spent radioactive ion-exchange resins produced in the nuclear industry, Prog. Nucl. Engery, 78 (2015) 47-55, https://doi.org/10.1016/j.pnucene.2014.08.003.

[12] J. Kim, B.K. Singh, W. Um, Effect of ion exchange resin particle size on homogeneity and leachability of Cs and Co in polymer waste form, RSC Adv., 11 (2021) 2729-2732, https://doi.org/10.1039/d0ra09669e.

[13] N.H. Hamodi, Y. Iqbal, Immobilization of Spent Ion Exchange Resin Arising From Nuclear Power Plants: An Introduction, J. Pak. Mater. Soc., 3 (2009) 7-18.

[14] B.K. Singh, N.S. Mahzan, N.S. Abdul Rashid, S.A. Isa, M.A. Hafeez, S. Saslow, G. Wang, C. Mo, W. Um, Design and Application of Materials for Sequestration and Immobilization of $^{99}$Tc, Environ. Sci. Technol., 57 (2023) 6776-6798, https://doi.org/10.1021/acs.est.3c00129.

[15] J.L. Provis, J.S.J. Van Deventer, 2009. Geopolymers: structures, processing, properties and industrial applications. Woodhead Publishing, Cambridge

[16] P. Duxson, A. Fernandez-Jimenez, J.L. Provis, G.C. Lukey, A. Palomo, J.S.J. van Deventer, Geopolymer technology: the current state of the art, J. Mater. Sci., 42 (2007) 2917-2933, https://doi.org/10.1007/s10853-006-0637-z.

[17] B. Kim, B. Lee, C.M. Chon, S. Lee, Compressive Strength Properties of Geopolymers from Pond Ash and Possibility of Utilization as Synthetic Basalt, J. Korean Ceram., 56 (2019) 365-373, https://doi.org/10.4191/kcers.2019.56.4.03.

[18] J. Ahn, W.S. Kim, W. Um, Development of metakaolin-based geopolymer for solidification of sulfate-rich HyBRID sludge waste, J. Nucl. Mater., 518 (2019) 247-255, https://doi.org/10.1016/j.jnucmat.2019.03.008.

[19] N. Kozai, J. Sato, T. Osugi, I. Shimoyama, Y. Sekine, F. Sakamoto, T. Ohnuki, Sewage sludge ash contaminated with radiocesium: Solidification with alkaline-reacted metakaolinite

(geopolymer) and Portland cement, J. Hazard. Mater., 416 (2021) 125965, https://doi.org/10.1016/j.jhazmat.2021.125965.

[20] V. Cantarel, F. Nouaille, A. Rooses, D. Lambertin, A. Poulesquen, F. Frizon, Solidification/stabilisation of liquid oil waste in metakaolin-based geopolymer, J. Nucl. Mater., 464 (2015) 16-19, https:// doi.org/10.1016/j.jnucmat.2015.04.036.

[21] J. Lee, B. Kim, J. Kang, J. Kang, W.-S. Kim, W. Um, Comparative Study Between Geopolymer and Cement Waste Forms for Solidification of Corrosive Sludge, J. Nucl. Fuel Cycle Waste Technol., 18 (2020) 465-479, https://

[22] B. Kim, J. Lee, J. Kang, W. Um, Development of geopolymer waste form for immobilization of radioactive borate waste, J. Hazard. Mater., 419 (2021) 126402, https://doi.org/10.1016/j.jhazmat.2021.126402.

[23] X. Niu, Y. Elakneswaran, C.R. Islam, J.L. Provis, T. Sato, Adsorption behaviour of simulant radionuclide cations and anions in metakaolin-based geopolymer, J. Hazard. Mater., 429 (2022) 128373, https://doi.org/10.1016/j.jhazmat.2022.128373.

[24] W.H. Lin, H.Y. Chen, C.P. Huang, Performance study of ion exchange resins solidification using metakaolin-based geopolymer binder, Prog. Nucl. Engery, 129 (2020) 103508, https://doi.org/10.1016/j.pnucene.2020.103508.

[25] H. Hamdane, M. Oumam, H.S. Mhamdi, A. Bouih, T. El Ghailassi, R. Boulif, J. Alami, B. Manoun, H. Hannache, Elaboration of geopolymer package derived from uncalcined phosphate sludge and its solidification performance on nuclear grade resins loaded with (134)Cs, Sci. Total Environ., 857 (2023) 159313, https://doi.org/10.1016/j.scitotenv.2022.159313.

[26] G.B.A. Terbang, Immobilization of spent ion exchange resin from PUSPATI TRIGA reactor using fly ash-based geopolymer, Malays. J. Anal. Sci., 19 (2015) 472-480.

[27] W.H. Lee, T.W. Cheng, Y.C. Ding, K.L. Lin, S.W. Tsao, C.P. Huang, Geopolymer

technology for the solidification of simulated ion exchange resins with radionuclides, J. Environ. Manage., 235 (2019) 19-27, https://doi.org/10.1016/j.jenvman.2019.01.027.

[28] M. Zribi, S. Baklouti, Investigation of Phosphate based geopolymers formation mechanism, J. Non-Cryst. Solids., 562 (2021) 120777, https://doi.org/10.1016/j.jnoncrysol.2021.120777.

[29] H. Lin, H. Liu, Y. Li, X.M. Kong, Properties and reaction mechanism of phosphoric acid activated metakaolin geopolymer at varied curing temperatures, Cem. Concr. Res., 144 (2021) 106425, https:// doi.org/10.1016/j.cemconres.2021.106425.

[30] D.S. Perera, J.V. Hanna, J. Davis, M.G. Blackford, B.A. Latella, Y. Sasaki, E.R. Vance, Relative strengths of phosphoric acid-reacted and alkali-reacted metakaolin materials, J. Mater. Sci., 43 (2008) 6562-6566, https://doi.org/10.1007/s10853-008-2913-6.

[31] L.P. Liu, X.M. Cui, Y. He, S.D. Liu, S.Y. Gong, The phase evolution of phosphoric acid-based geopolymers at elevated temperatures, Mater. Lett., 66 (2012) 10-12, https://doi.org/10.1016/j.matlet.2011.08.043.

[32] American National Standard, Measurement of the Leachability of Solidified Low-Level Radioactive Wastes by a Short-Term Test Procedure, 1986. ANSI/ANS-16.1.

[33] K. Suzuki, Y. Ono, Leaching characteristics of stabilized/solidified fly ash generated from ash-melting plant, Chemosphere, 71 (2008) 922–932, https://doi.org/10.1016/j.chemosphere.2007.11.002

[34] R.O. Abdel Rahman, A.A. Zaki, Assessment of the leaching characteristics of incineration ashes in cement matrix, Chem. Eng. J., 155 (2009) 698–708. https://doi.org/10.1016/j.cej.2009.09.002

[35] B.Y. Li, Y.M. Zhang, D.X. Ma, Z.Y. Xing, T.L. Ma, Z. Shi, X.L. Ji, S.Q. Ma, Creation of a new type of ion exchange material for rapid, high-capacity, reversible and selective ion

exchange without swelling and entrainment, Chem. Sci., 7 (2016) 2138-2144, https://doi.org/10.1039/c5sc04507j.

[36] M. Neji, B. Bary, P. Le Bescop, N. Burlion, Swelling behavior of ion exchange resins incorporated in tri-calcium silicate cement matrix: I. Chemical analysis, J. Nucl. Mater. 467 (2015) 544-556, https://doi.org/10.1016/j.jnucmat.2015.10.013.

[37] V. Mathivet, J. Jouin, M. Parlier, S. Rossignol, Control of the alumino-silico-phosphate geopolymers properties and structures by the phosphorus concentration, Mater. Chem. Phys. 258 (2021) 123867, https://doi.org/10.1016/j.matchemphys.2020.123867.

[38] M.T. Yamchelou, D. Law, R. Brkljača, J. Li, I. Patnaikuni, Pre-treatment impact on the disposition of water in clay-based geopolymer, Open Ceram., 5 (2021) 100053, https://doi.org/10.1016/j.oceram.2020.100053.

[39] G.W. Liang, W. Yao, A.M. She, New insights into the early-age reaction kinetics of metakaolin geopolymer by 1H low-field NMR and isothermal calorimetry, Cem. Concr. Compos. 137 (2023) 104932, https://doi.org/10.1016/j.cemconcomp.2023.104932.

[40] A.C. Muller, K.L. Scrivener, A.M. Gajewicz, P.J. McDonald, Densification of C–S–H measured by 1H NMR relaxometry, J. Phys. Chem. C, 117 (2013) 403-412, https://doi.org/10.1021/jp3102964.

[41] L. Liu, Z. He, X. Cai, S. Fu, Application of low-field NMR to the pore structure of concrete, Appl. Magn. Reson. 52 (2021) 15-31, https://doi.org/10.1007/s00723-020-01229-70

[42] A. Sadiq, S. Fakhi, T.E. Ghailassi, Z. Faiz, A. Bouih, H. Hannache, Contribution of Metakaolin to the Confinement of Spent Resins by Cementation, J. Hazard., Toxic Radioact. Waste., 26 (2022) 04022018, https://doi.org/10.1061/(ASCE)HZ.2153-5515.0000704.

[43] F. Vodák, V. Vydra, K. Trtík, O. Kapičková, Effect of gamma irradiation on properties of hardened cement paste, Materials and structures, 44, (2019), 101-107,

ttps://doi.org/10.1617/s11527-010-9612-x.

[44] D. Lambertin, C. Boher, A. Dannoux-Papin, K. Galliez, A. Rooses, F. Frizon, Influence of gamma ray irradiation on metakaolin based sodium geopolymer, J. Nucl. Mater. 443 (2013) 311-315, https://doi.org/10.1016/j.jnucmat.2013.06.044.

[45] R.R. Lloyd, J.L. Provis, J.S.J. van Deventer, Pore solution composition and alkali diffusion in inorganic polymer cement, Cem. Concr. Res., 40 (2010) 1386-1392, https://doi/org/10.1016/j.cemconres.2010.04.008.

[46] G. Bykov, A. Gordeev, T. Yurik, B. Ershov, https://doi.org/10.1134/S0018143908030041, High Energy Chem., 42 (2008) 211-214.

[47] C. Nobouassia Bewa, H.K. Tchakouté, D. Fotio, C.H. Rüscher, E. Kamseu, C. Leonelli, Water resistance and thermal behavior of metakaolin-phosphate-based geopolymer cements, J. Asian Ceram. Soc. 6 (2018) 271-283, https://doi.org/10.1080/21870764.2018.1507660

[48] C. Fernandez-Lorenzo, L. Esquivias, P. Barboux, J. Maquet, F. Taulelle, Sol-gel synthesis of $SiO_2$-$P_2O_5$ glasses, J. Non-Cryst. Solids., 176 (1994) 189-199, https://doi.org/10.1016/0022-3093(94)90077-9.

[49] B. Kim, S.Y. Shin, J. Kang, W. Um, Waste acceptance criteria testings of a phosphate-based geopolymer waste form to immobilize radioactive borate waste, J. Nucl. Mater., 586 (2023), 154671, https://doi.org/10.1016/j.jnucmat.2023.154671.

[50] T. Dong, S.B. Xie, J.S. Wang, G.D. Zhao, Q.C. Song, Solidification and Stabilization of Spent TBP/OK Organic Liquids in a Phosphate Acid-Based Geopolymer, Sci. Technol. Nucl., 2020 (2020), https://doi.org/10.1155/2020/8094205.

[51] M. Mamo, D. Ginting, R. Renken, B. Eghball, Stability of ion exchange resin under freeze-thaw or dry-wet environment, Soil. Sci. Soc. Am. J. 68 (2004) 677-681, https://doi.org/10.2136/sssaj2004.6770.

[52] Q. Tian, K. Sasaki, A novel composite of layered double hydroxide/geopolymer for co-immobilization of $Cs^+$ and $SeO_4^{2-}$ from aqueous solution, Sci. Total. Environ., 695 (2019) 133799, https://doi.org/10.1016/j.scitotenv.2019.133799.

[53] C.Y. Bai, A. Conte, P. Colombo, Open-cell phosphate-based geopolymer foams by frothing, Mater. Lett., 188 (2017) 379-382, https://doi.org/10.1016/j.matlet.2016.11.103.

[54] J.N.Y. Djobo, Moustapha, L.P.T. Ndjonnou, K.K. Etame, D. Stephan, The role of curing temperature and reactive aluminum species on characteristics of phosphate geopolymer, RSC Adv., 12 (2022) 29653-29665, https://doi.org/10.1039/d2ra04562a.

[55] S.C. Park, H.R. Cho, J.H. Lee, H.Y. Yang, O.B. Yang, A study on adsorption and desorption behaviors of $^{14}C$ from a mixed bed resin, Nucl. Eng. Technol., 46 (2014) 847-856, https://doi.org/10.5516/NET.06.2014.088.

[56] X. Chen, H. Ma, C. Luo, T. Zhou, Recovery of valuable metals from waste cathode materials of spent lithium-ion batteries using mild phosphoric acid, J. Hazard. Mater., 326 (2017) 77-86, https://doi.org/10.1016/j.jhazmat.2016.12.021.

[57] M.L.Y. Yeoh, S. Ukritnukun, A. Rawal, J. Davies, B.J. Kang, K. Burrough, Z. Aly, P. Dayal, E.R. Vance, D.J. Gregg, P. Koshy, C.C. Sorrell, Mechanistic impacts of long-term gamma irradiation on physicochemical, structural, and mechanical stabilities of radiation-responsive geopolymer pastes, J. Hazard. Mater., 407 (2021) 124805, https://doi.org/10.1016/j.jhazmat.2020.124805.

[58] P. Perez-Cortes, I. Garcia-Lodeiro, M.C. Alonso, F. Puertas, Cementation of spent radioactive ion-exchange resin ashes using alkali-activated cements: Physicochemical and structural changes. Cem. Concr. Compos., 149, (2024) 105517, https://doi.org/10.1016/j.cemconcomp.2024.105517.

[59] X. Niu, Y. Elakneswaran, N. Hiroyoshi, Surface chemistry and radionuclide anion

immobilisation potential of phosphoric acid-activated metakaolin-based geopolymers, Cem. Concr. Res., (2024) 181, 107549. https://doi.org/10.1016/j.cemconres.2024.107549.

Table 1. Concentration of simulant acidic liquid waste

| Component | Concentration (ppm) |
|---|---|
| Fe | 6500 |
| Cr | 5000 |
| Mn | 5000 |
| Ni | 5000 |
| Co | 700 |
| Cs | 300 |
| Sr | 700 |

Table 2. Mix designs of P-GP waste form

| Sample | L/S ratio | IERs loading (wt%) | curing conditions |
|---|---|---|---|
| 1.2G0 | 1.2 | 0 | RT for 5d + 60 ℃ for 1d |
| 1.2G10 | | 10 | |
| 1.2G20 | | 20 | |
| 1.2G30 | | 30 | |
| 1.2G40 | | 40 | |
| 1.2G50 | | 50 | |
| 1.0G10 | 1.0 | 10 | |
| 1.0G20 | | 20 | |
| 0.7G30 | 0.7 | 30 | |
| 0.7G40 | | 40 | |
| 0.7G50 | | 50 | |

Table 3. 7-day compressive strength of P-GP waste form with different waste loadings

| Sample | IERs loading (wt%) | 7-days compressive strength (MPa) |
|---|---|---|
| 1.2G0 | 0 | 73 ± 3.03 |
| 1.2G10 | 10 | 17 ± 0.86 |
| 1.2G20 | 20 | 13 ± 1.35 |
| 1.2G30 | 30 | 8 ± 0.26 |
| 1.2G40 | 40 | 5 ± 0.28 |
| 1.2G50 | 50 | 3 ± 0.31 |
| 1.0G10 | 10 | 23 ± 1.26 |
| 1.0G20 | 20 | 15 ± 0.13 |
| 0.7G30 | 30 | 10 ± 0.28 |
| 0.7G40 | 40 | 7 ± 0.09 |
| 0.7G50 | 50 | 5 ± 0.10 |

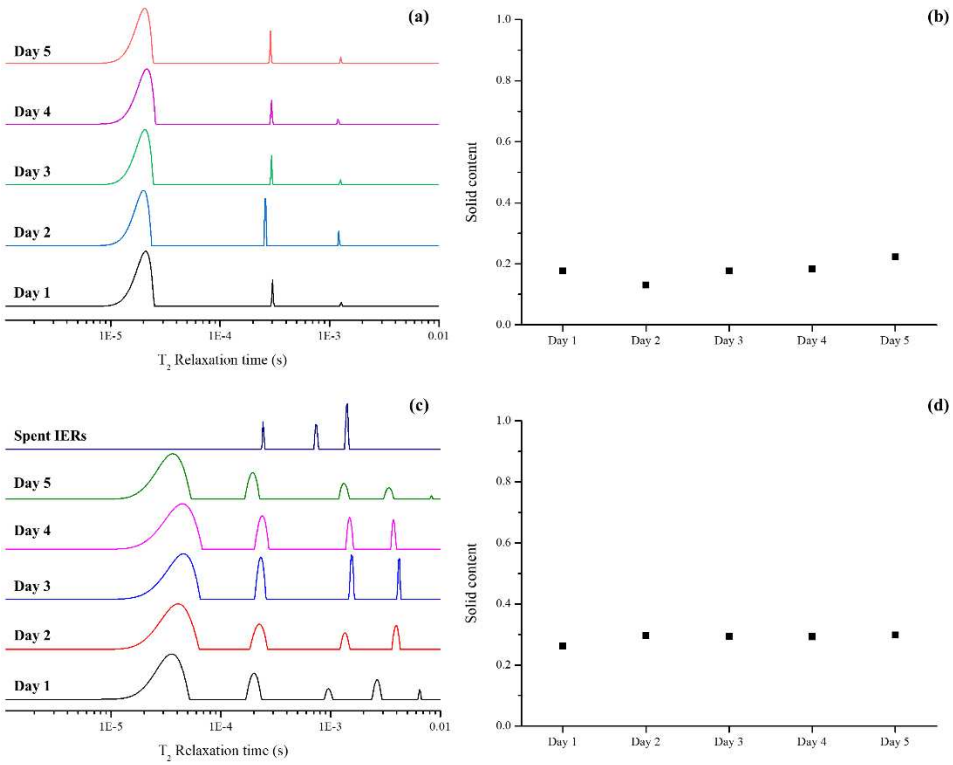


Figure 1. $T_2$ relaxation time spectra and solid content; pure geopolymer with an L/S ratio of 2.0 (a and b) and 0.7G40 P-GP waste form (c and d)

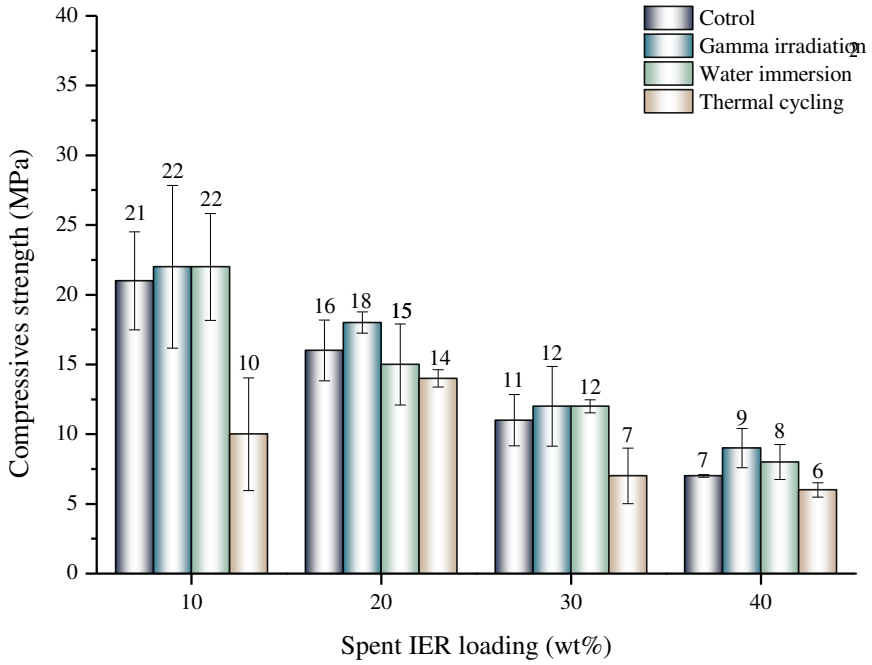


Figure 2. Compressive strength of P-GP waste form after the waste acceptance criteria testings

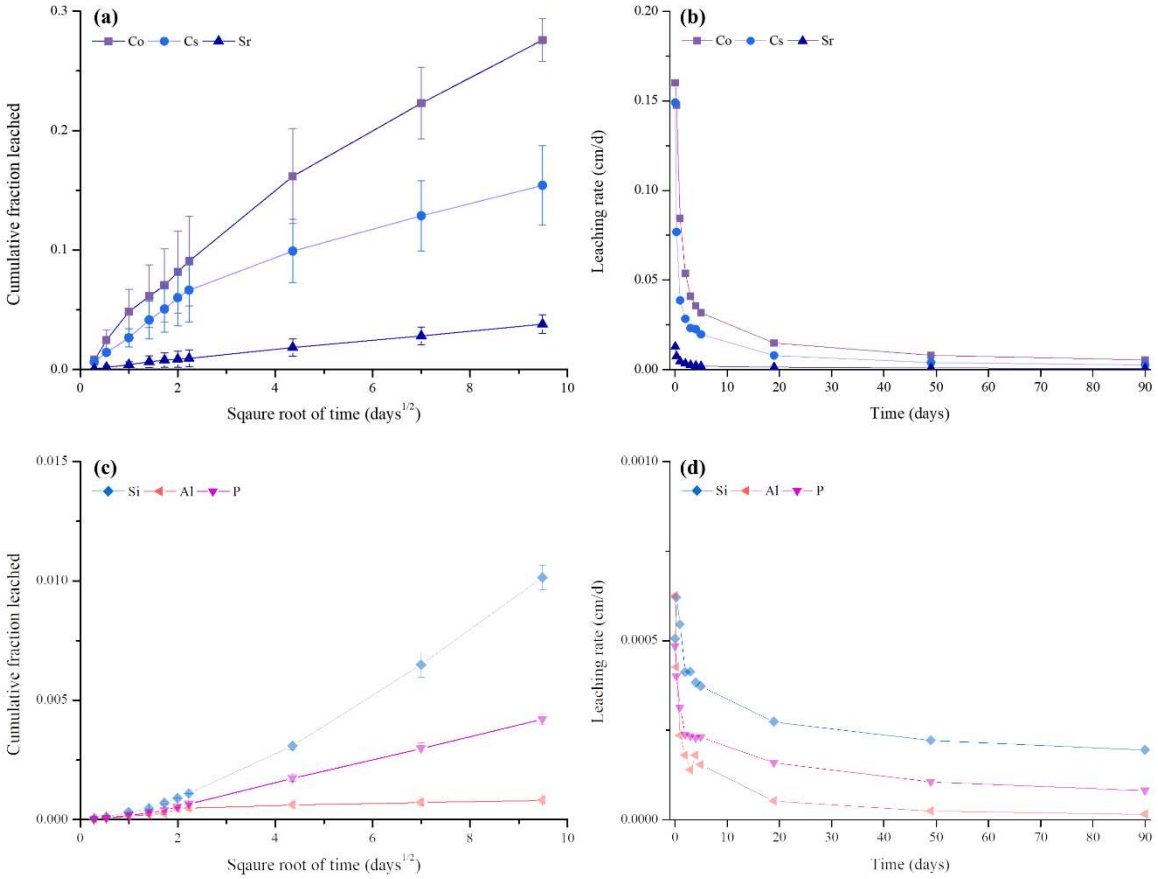

Figure 3. The 90-days leaching test results of 0.7G40 P-GP waste form; cumulative fraction leached and leaching rate of Co, Cs, and Sr (a and b) and major elements (Si, Al, and P) of 0.7G40 P-GP waste form (c and d)

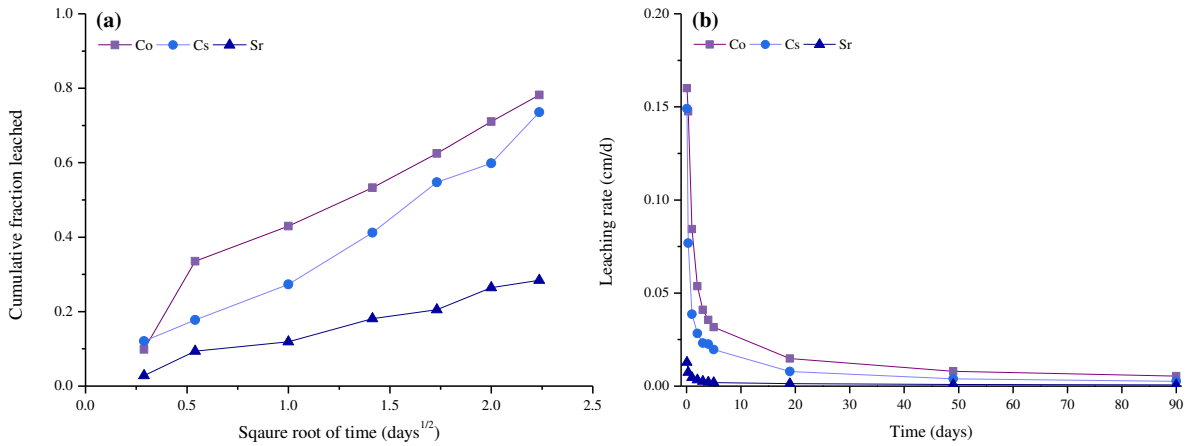


Figure 4. Acid immersion test results of simulant spent IERs without geopolymer waste form; cumulative fraction leached (a) and leaching rate (b)

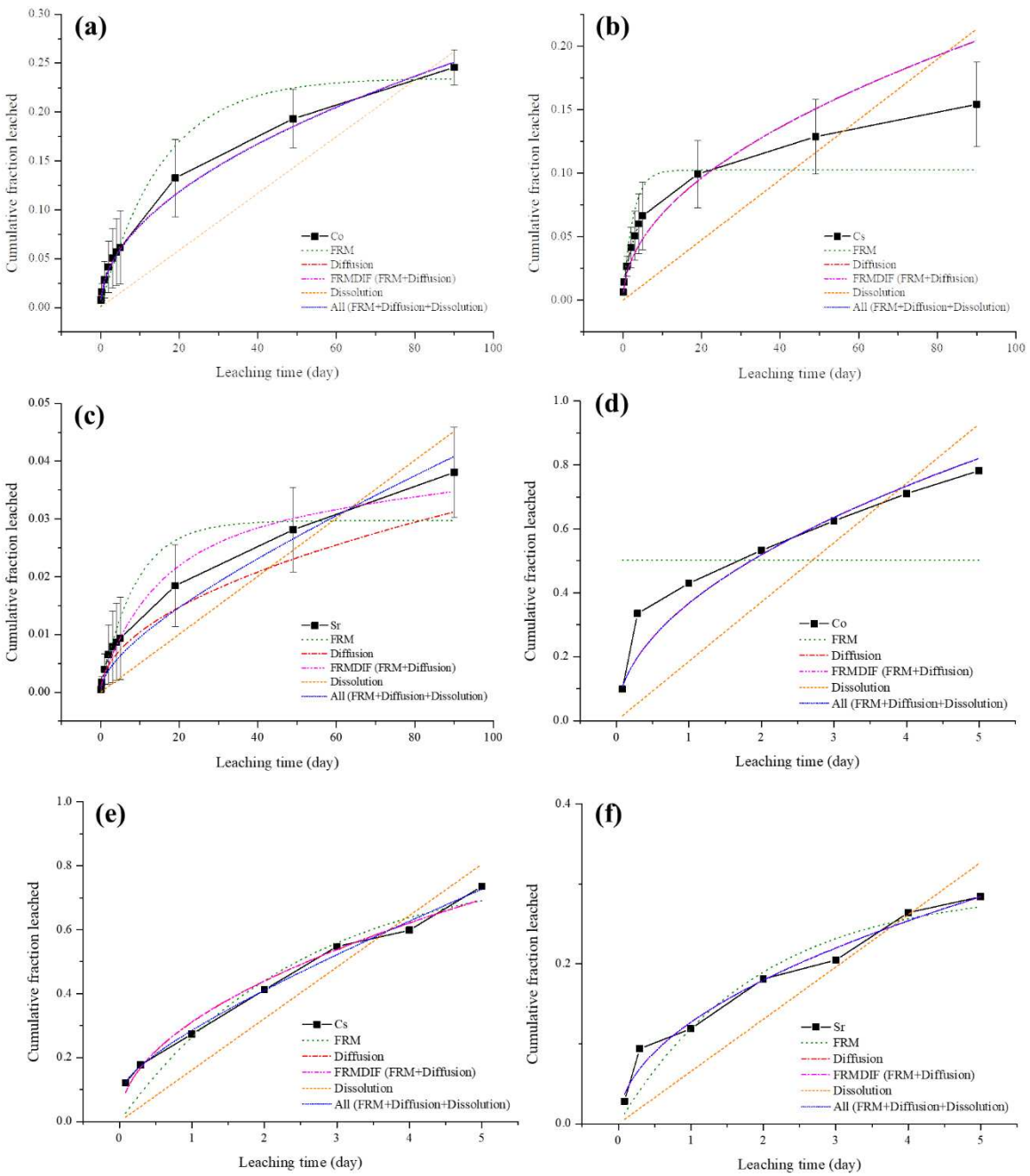


Figure 5. Kinetic model fitting to the experimental data for 0.7G40 geopolymer (a-c) and acid immersion test (d-f)

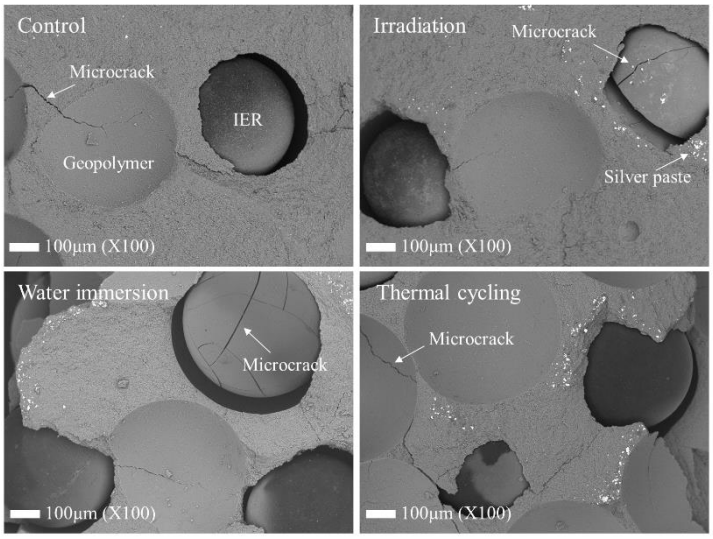


Figure 6. Microstructure of 0.7G40 P-GP waste form after various waste acceptance criteria testings

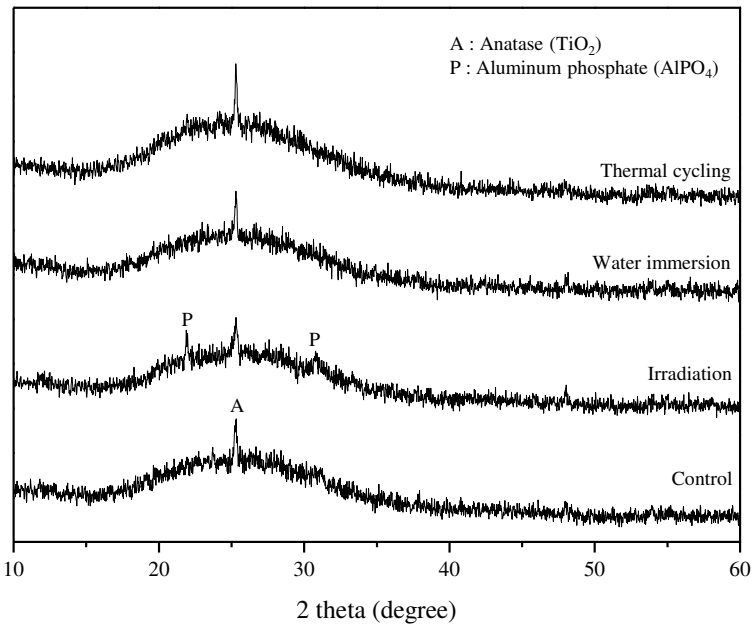


Figure 7. XRD results of 0.7G40 P-GP waste form after the waste acceptance criteria testings

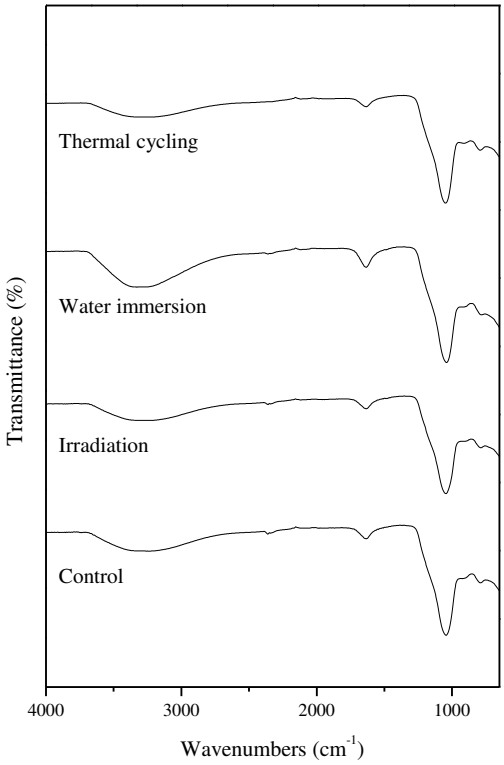


Figure 8. FT-IR results of 0.7G40 P-GP waste form after the waste acceptance criteria testings